*Earth and Planetary Science Letters*, 119 (1993) 103–119
Elsevier Science Publishers B.V., Amsterdam



[MK]

# A 4300 year strontium isotope record of estuarine paleosalinity in San Francisco Bay, California

B. Lynn Ingram [a,b] and Donald J. DePaolo [a]

[a] *Center for Isotope Geochemistry, Department of Geology and Geophysics, University of California, and Earth Sciences Division, Lawrence Berkeley Laboratory, Berkeley, California 94720, USA*

[b] *Center for Accelerator Mass Spectrometry, Lawrence Livermore National Laboratory, PO Box 808, L-397, Livermore, California 94550, USA*

Received January 15, 1993; revision accepted June 2, 1993

ABSTRACT

Strontium isotopic compositions of carbonate mollusk shells from estuarine sediments cored beneath San Francisco Bay are used to derive a record of mean annual salinity and average freshwater inflow to the estuary for intervals during the past 4300 yrs. The large difference in the $^{87}Sr/^{86}Sr$ ratio between seawater (0.7092) and the average freshwater entering the estuary (0.7065) produces a correlation between $^{87}Sr/^{86}Sr$ and salinity in bay waters that can be detected with high-precision measurements. Paleosalinity is inferred from the $^{87}Sr/^{86}Sr$ ratio measured in fossil carbonate shells of bivalves preserved in the sediment. Because salinity in San Francisco Bay is primarily controlled by the freshwater inflow from the Sacramento and San Joaquin rivers, the paleosalinity record can be converted to a paleodischarge record using a transfer function derived from historical data.

Salinity data are referenced to modern values estimated for the estuary after correcting for the lower discharge caused by diversion since 1850 A.D. Data are presented from Richardson Bay, located near the estuary mouth (modern mear arrival salinity (MAS) of ca. 24‰), and from San Pablo Bay, located about 30 km upstream (modern MAS of ca. 18–20‰). For Richardson Bay, the data cover the periods 0–600 yrs B.P. and 2200–4300 yrs B.P., based on radiocarbon dating. For San Pablo Bay, the periods 0–130 yrs B.P. and 2500–2800 yrs B.P. are represented.

The Richardson Bay data indicate extended periods of low salinity relative to modern, indicating higher freshwater inflow, at ca. 80, 220, 310, 440–500, 3100–3400 and 4300 yrs ago. The data indicate high salinity relative to modern, hence lower freshwater inflow, at about 40, 140–210, 270, 2100 and 3450–3700 yrs B.P. For San Pablo Bay, where salinity resolution is better, salinity was lower than modern during the period at ca. 50 and 2550–2650 yrs B.P., and higher than modern at ca 90–110, 155 and 2510–2530 yrs B.P. The data suggest that mean annual discharge to San Francisco Bay typically varies between values that are below the modern value (600 $m^3/s$) and values 2 to 3 times as high; the average paleosalinity is typically substantially lower than the modern values. The 4300 yr average freshwater inflow is estimated to be $\geqslant 1200 \pm 200$ $m^3/s$. The record indicates that quasi-cyclic variations in mean annual discharge occur naturally with a period of about 200 yrs or less.

## 1. Introduction

An important input to water resource assessment is the natural history of long-term precipitation and streamflow. For most of the western United States, historical stream-flow records are no longer than 100 years. Proxy methods for extending paleo-precipitation and stream flow records farther back in time are therefore critical for documenting the natural variability and long-term average precipitation. Methods for evaluating paleo-precipitation include treering widths [1–4], treeline variations [5], fluctuations in lake levels [6], and Sr isotopic studies of estuarine salinity [7,8]. In this study we use the Sr isotope method to determine the paleosalinity of, and therefore paleo-river discharge into, the San Francisco Bay estuary for much of the past 4500 yrs. Paleosalinity is a particularly useful proxy for paleo-precipitation in California because the streams that discharge into San Francisco Bay and determine its salinity drain a large area (40% of California, or 162,000 $km^2$) and average the precipitation both temporally and spatially [9].

Streamflow in the northwestern United States also has broader climatic significance, in that it is linked to large-scale atmospheric circulation over the North Pacific [9].

Ninety percent of the freshwater that enters San Francisco Bay comes from the Sacramento–San Joaquin watershed (Fig. 1). The waters of the bay are mixtures of saline ocean water and freshwater from the rivers. River discharge is the primary control on salinity in San Francisco Bay [10]; discharge and salinity vary seasonally over a substantial range and also on longer timescales with climatic changes. The salinity of the oceanic component of San Francisco Bay waters also varies seasonally, with high salinity during spring upwelling, but the seawater variations are negligible compared to those caused by variations in freshwater inflow [10].

## 2. Quaternary sea level and sedimentation

The sediments beneath San Francisco Bay represent alternating estuarine and fluvial deposition over the past 450,000 yrs or more [11–13], reflecting sea-level changes associated with fluctuations in the volume of continental ice. Modern San Francisco Bay began forming at the end of the last glacial period (10,000 yrs ago), when sea level rose above the level of the Golden Gate, which is about 50 m below present sea level (Fig. 2 [11,12]). A Holocene sea level record, constructed from depths and $^{14}C$ ages of marsh plants recovered

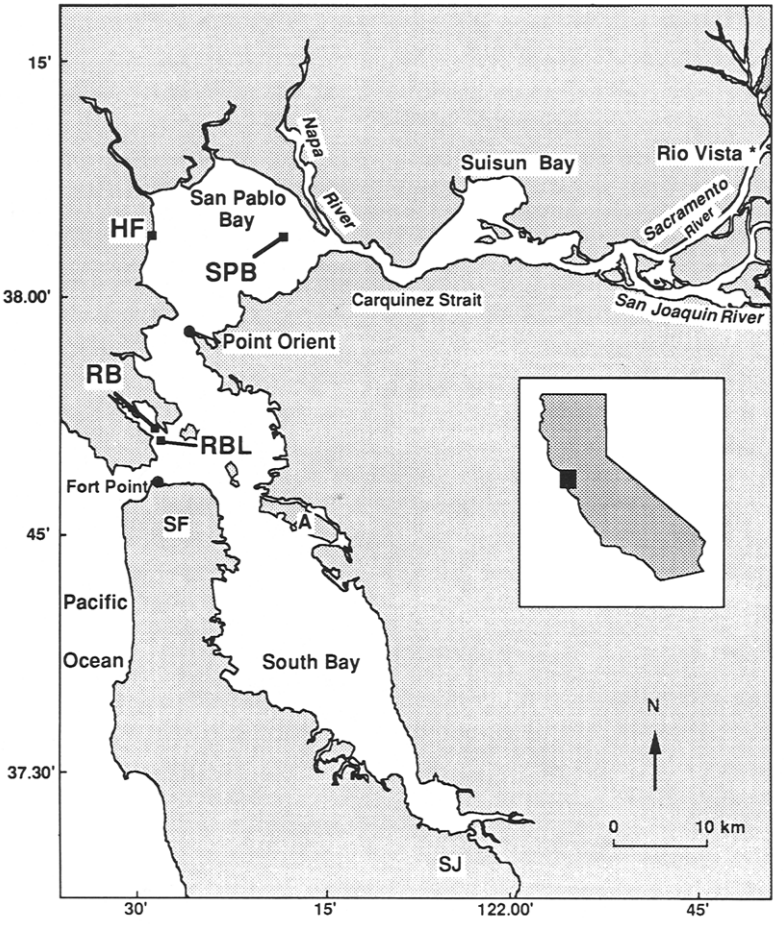


Fig. 1. Map of San Francisco Bay and delta, showing location of two 2 m gravity cores (*RB* from Richardson Bay and *SPB* from San Pablo Bay) and 10 m long cores (*HF* from Hamilton Field, San Pablo Bay and *RBL* from Richardson Bay) used in this study. Salinity monitoring stations (Fort Point and Point Orient) are also shown.

from sediment cores [11,12] corresponds closely to the global sea-level curve of Fairbanks (Fig. 2 [14]). We infer from the sea-level data that the volume of San Francisco Bay has been controlled almost entirely by eustatic sea level and intra-estuarine sedimentation rather than by tectonic uplift or subsidence over the past 10,000 yrs.

Sediment entering San Francisco Bay (primarily silt and clay carried in suspension), like the freshwater inflow, comes primarily from the Sacramento–San Joaquin drainage basin [15]. Most of the sediment enters the bay during the period of high river inflow associated with winter rainfall and spring snowmelt [15], and is deposited in broad, shallow regions of northern San Francisco Bay, where current velocities are low relative to the channels. The sediment accumulation rate varies greatly within the estuary, but the average sedimentation rate over the past 5000 yrs for the south bay and central bay is likely to be between the values of 1.0–1.2 mm/yr measured in the south bay [11], and the 2.6 mm/yr measured in Richardson Bay [16]; sedimentation rates are generally somewhat higher in the northern part of the bay closer to the delta [15].

Time resolution within the sediments depends on the depth of mixing (bioturbation) by burrowing organisms relative to the sediment accumulation rate. The depth of bioturbation in the Holocene sediments of San Francisco Bay is between 5 and 30 cm, although most sediments are not bioturbated below 15 cm [H.E. Clifton, pers. commun.]. For a bioturbation depth of 10 cm and a sedimentation rate of 2 mm/yr the sedimentary record in San Francisco Bay would be a running average with an integration window of about 50 yrs. Better time resolution would be possible in regions with higher sediment accumulation rates, such as in San Pablo and Suisun bays. The seasonal and tidal variations of the paleosalinity record are smoothed by bioturbation.

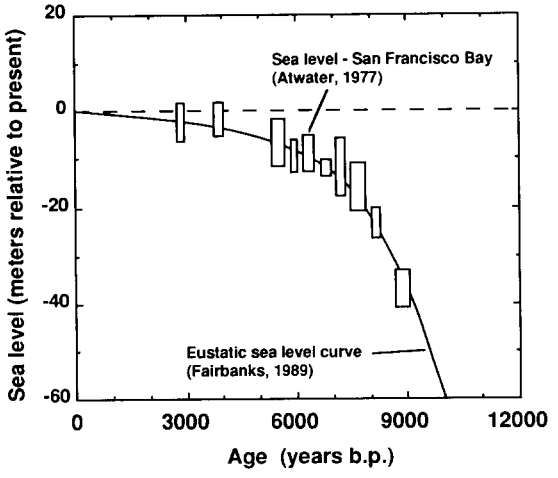


Fig. 2. Sea-level curve for the past 10,000 yrs, showing both the eustatic sea level recorded in Barbados coral reefs [14], and sea level recorded in San Francisco Bay sediments [11].

## 3. Method

As described by Ingram and Sloan [8], the Sr isotope method is based on the relationship between salinity and $^{87}Sr/^{86}Sr$ in the water. This relationship is established using two approaches, which give good agreement. One approach is to measure the Sr concentration and Sr isotopic ratio of river waters entering the bay, and to use this and the properties of seawater to calculate the $^{87}Sr/^{86}Sr$–salinity relationship. The $^{87}Sr/^{86}Sr$ ratio of the mixture ($R_{mix}$) is a function of the $^{87}Sr/^{86}Sr$ ratio and concentration of Sr in the river water ($R_r$ and $C_r$) and ocean water ($R_o$ and $C_o$) end members:

$$R_{mix} = [C_r R_r f + C_o R_o (1-f)]/C_{mix}$$

where $C_{mix}$ is the concentration of Sr in the estuarine water, and $f$ is the fraction of river water [10]. To a good approximation, salinity ($S_{mix}$) is given by:

$$S_{mix} \approx (1-f) S_o$$

where $S_o$ is the salinity of ocean water.

To verify the calculated relationship, the $^{87}Sr/^{86}Sr$ and salinity of modern bay water were measured (Figs. 3 and 4 [7,8]). Also shown in Figs. 3 and 4 are calculated mixing trajectories and the data for river water and estuarine water. In Figure 3 the $^{87}Sr/^{86}Sr$ ratios are plotted against 1/Sr; on this plot mixing trajectories are straight lines (Fig. 3). The data for the river waters of the Sacramento and San Joaquin rivers near the delta are nearly colinear with the seawater value and the estuarine water data (line *b* in Fig. 3). The colinearity of the seawater composition and the data from the mouths of both rivers indicate that varying the proportions of freshwater contributed

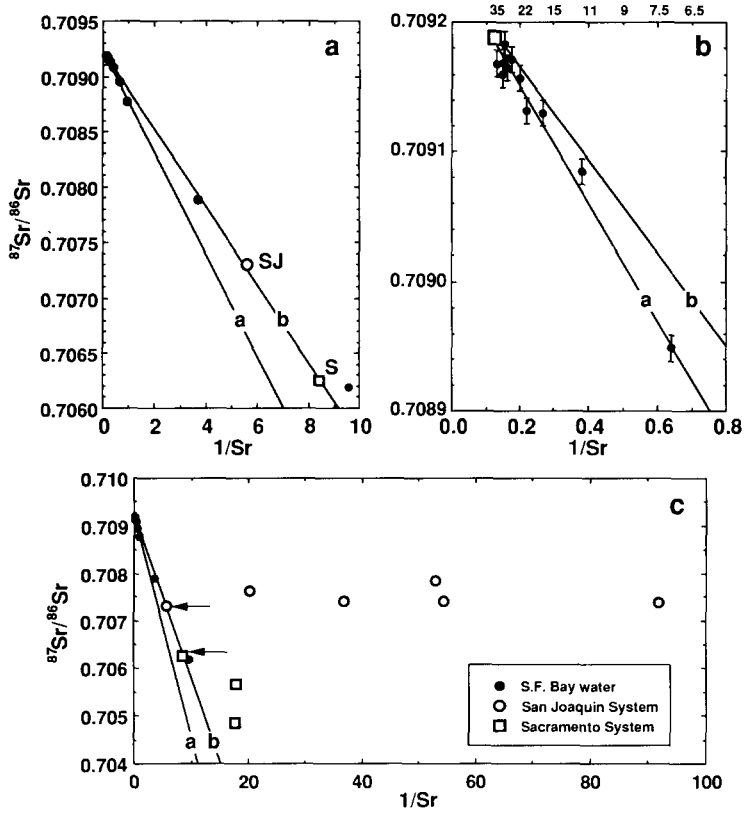


Fig. 3. $^{87}Sr/^{86}Sr$ versus $1/Sr$ in estuarine and river waters [7,8]. (a) Estuarine water data and measurements of river water from near the mouths of the Sacramento River (*S*) and the San Joaquin River (*SJ*) showing the near-colinearity of the river values and the seawater value. Line *b* connects the seawater and river data; line *a* is an approximate fit to the high-salinity estuarine water data. (b) Expanded view of the estuarine water data; numbering across the top of the figure is salinity (permil). (c) Data from (a) together with data from tributaries of the Sacramento and San Joaquin rivers.

by the Sacramento River versus the San Joaquin River will not change the $^{87}Sr/^{86}Sr$–salinity relationship in the estuarine waters.

The Sr isotopic data are plotted against salinity in Fig. 4. The light lines show the relationship calculated from the measured seawater and riverine end-member compositions. The calculated lines do not exactly fit the estuarine data. The heavy line is a fit to the estuarine water data, which require a riverine Sr concentration of 160 ppb, somewhat higher than the average of the measured values in the streams (130 ppb). The heavy line is the relationship used to calculate the salinities listed in Tables 2 and 3. Use of the fit to the estuarine water data, as opposed to the mixing lines for measured seawater and river waters, may cause our calculated salinities to be slightly high.

The streams closer to the headwaters of the San Joaquin system have similar $^{87}Sr/^{86}Sr$ values, but much lower Sr concentrations, than those from near the mouth of the San Joaquin River (Fig. 3). The same effect is observed for the Sacramento system, but with a much narrower range of Sr concentrations than for the San Joaquin river. If water with Sr concentration more similar to that of the headwater rivers were entering the bay (such as during periods of particularly high discharge), the relationship between $^{87}Sr/^{86}Sr$ and salinity would change from that shown in Fig. 4. The direction of this change is such that calculated salinity would be too high. Although there is one estuarine water data point that falls below line *b* in Fig. 3, there appears in general to be little likelihood of *underestimating* paleosalinity using the estuarine water trend. We therefore

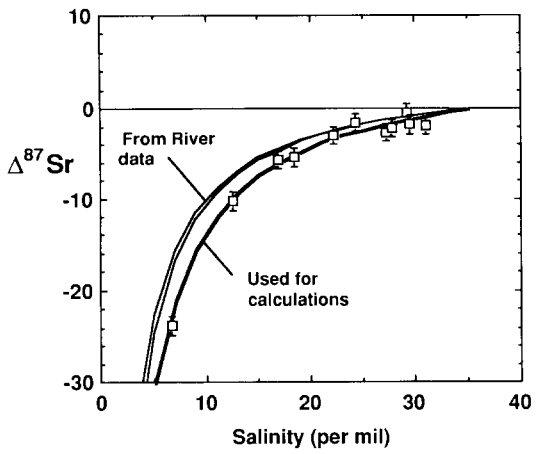


Fig. 4. Relationship between $\Delta^{87}Sr$ and salinity in estuarine water [from 7,8], showing calculated mixing curves for addition of measured San Joaquin and Sacramento river water end member (light lines), and for addition of a model river water component with properties selected to fit the estuarine water data (heavy line). The $\Delta^{87}Sr$ values of the estuarine samples are about 1 unit higher than those reported by Ingram and Sloan [8]; the values shown here are based on a re-evaluation of the seawater carbonate standard (EN-1) results for the time period during which the isotopic measurements were made.

expect that where our inferred salinities differ from the true paleosalinity, these inferred salinities are most likely to be *too high*, and therefore the inferred river discharge would be *too low*. We are currently measuring both river and estuarine water throughout the seasonal cycle to evaluate any second-order effects on the riverine $^{87}Sr/^{86}Sr$ ratio and Sr concentration, associated with changes in discharge volume and evaporation [cf. 17].

## 4. Sample descriptions

The fossil shells used for this study were taken from sediment cores taken from beneath San Francisco Bay between the Golden Gate and the delta (Fig. 1). The cores include two 2.0–2.5 m, 15 cm diameter gravity cores (one each from Richardson Bay and San Pablo Bay), an 11 m core with 10 cm diameter from Richardson Bay (cored in 1991 by the U.S. Geological Survey), and an 11 m, 4 cm diameter core from San Pablo Bay. Neither 11 m core sampled the upper 2.5 m of sediment. The long core from Richardson Bay was drilled from a slope near the main channel, in a water depth of about 12 m, and it was designed to sample from the depths of 2.5 m to 11 m. The San Pablo Bay long core was drilled in an infilled marsh on the west shore at Hamilton Field Airforce Base (Fig. 1). Due to coring difficulties and the effects of landfill, the upper 2.7 m of sediment was unusable in this core.

The sediments from the Hamilton Field core and San Pablo Bay gravity core are composed of varying amounts of fine clay and silt, fine sand, organic remains (plant fragments, wood and seeds from marsh plants), calcareous and agglutinated foraminifers, diatoms, ostracods, mollusks (whole shells and fragments of bivalves and small gastropods) and fish remains. The dominant bivalve that could be identified was *Macoma* species. The fine-grained sand and silt is composed of muscovite, quartz, feldspar and chrysotile (serpentine). The sediment from the Richardson Bay gravity core is composed of layered brown-gray silt and clay, with distinct layers rich in sand, mollusks (fragments and whole shells) or organic material. Identifiable mollusk shells included *Macoma* and *Ostrea*. Other fossils included foraminifers, fecal pellets, wood fragments, seeds, fish scales and otoliths, and diatoms. The sediments and fossils from the Richardson Bay long core are similar in composition to that of the gravity core, but contains less abundant fossil remains. Although many of the clam shells in all the cores were fragmented, the fragments were mostly large and angular with little or no signs of abrasion, suggesting minimal transport within the bay. Samples for isotopic analyses were selected from intervals which contained abundant fragments or whole mollusk shells.

## 5. Analytical methods

All but the long core from San Pablo Bay were cut in half lengthwise, with an archival half placed in storage at the U.S. Geological Survey. The sediment cores were initially subsampled at intervals of 10 cm (Richardson Bay gravity core), 20 cm (San Pablo Bay gravity core) and 30 cm (Hamilton Field core). The samples consisted of 2 cm thick sections yielding approximately 50 g of wet sediment. Mollusk shells (whole and fragments) and organic material (plant remains, seeds and

TABLE 1

Radiocarbon data for carbonate samples from San Francisco Bay sediment cores

| Sample Number | Depth (cm) | C-14 Age years | Calendar Age years | Corrected Age years* |
|---|---|---|---|---|
| **Richardson Bay Gravity Core** | | | | |
| RBGC-3 | 40 | <0 | 35 ± 5 | 35 ± 5 |
| RBGC-5 | 60 | 830 ± 60 | 725 ± 60 | 125 ± 60 |
| RBGC-7 | 80 | 580 ± 70 | 600 ± 70 | *0 ± 70* |
| RBGC-10 | 100 | 690 ± 60 | 670 ± 60 | *70 ± 60* |
| RBGC-12 | 130 | 890 ± 70 | 825 ± 105 | 225 ± 105 |
| RBGC-14 | 140 | 850 ± 110 | 750 ± 110 | *150 ± 110* |
| RBGC-17 | 170 | 670 ± 110 | 620 ± 70 | *20 ± 70* |
| RBGC-18 | 180 | 1100 ± 100 | 1040 ± 110 | 440 ± 110 |
| RBGC-20 | 195 | 1230 ± 70 | 1170 ± 100 | 570 ± 100 |
| **Richardson Bay Long Core** | | | | |
| RB-2.1A | 441 | 780 ± 80 | 690 ± 80 | 90 ± 80 |
| RB-2.1b | 460 | 1070 ± 70 | 970 ± 70 | 370 ± 70 |
| RB-2.2A | 526 | 2690 ± 60 | 2810 ± 60 | 2210 ± 60 |
| RB-2.3A | 666 | 3680 ± 80 | 4010 ± 80 | 3410 ± 80 |
| RB-2.5b | 815 | 3720 ± 70 | 4110 ± 70 | 3510 ± 70 |
| RB-2.6A | 849 | 3790 ± 100 | 4190 ± 100 | 3590 ± 100 |
| RB-2.9A | 1070 | 4390 ± 80 | 4920 ± 80 | 4320 ± 80 |
| **San Pablo Bay Gravity Core** | | | | |
| SPB-3A-2 | 20 | <0 | 35 ± 5 | 35 ± 5 |
| SPB-3A-3 | 40 | <0 | 35 ± 5 | 35 ± 5 |
| SPB-3A-9 | 150 | 730 ± 70 | 680 ± 70 | 130 ± 70 |
| SPB-3A-11 | 190 | 740 ± 60 | 680 ± 60 | 130 ± 60 |
| **San Pablo Bay long core (Hamilton field)** | | | | |
| HF-4cc | 270 | 1810 ± 120 | 1730 ± 150 | 1180 ± 150 |
| HF-5-2 | 334 | 2930 ± 60 | 3130 ± 80 | 2580 ± 80 |
| HF-6-1 | 395 | 2890 ± 90 | 3020 ± 90 | 2470 ± 90 |
| HF-9cc | 850 | 2820 ± 180 | 2985 ± 225 | 2435 ± 225 |
| HF-11-1 | 1003 | 3080 ± 80 | 3310 ± 90 | 2760 ± 90 |
| HF-11-2 | 1034 | 3070 ± 60 | 3320 ± 100 | 2770 ± 100 |

* Dates in italics are interpreted as being contaminated with modern carbon and are not used in determing sediment age. Corrected ages are younger than calendar ages by 600 yrs and 550 yrs, respectively, for Richardson Bay and San Pablo Bay samples, except for very young samples. Age calculations assume $\delta^{13}C = 0$, following Stuiver and Polach [37].

wood) were separated from the $>841$ $\mu$m fraction of each sample.

Organic and carbonate samples at 0.1–2 m intervals in the cores were selected for radiocarbon dating at the Center for Accelerator Mass Spectrometry (CAMS), at the Lawrence Livermore National Laboratory. Where possible, both carbonate (molluskan shells) and organic carbon (seeds and plants) were prepared from each level. The organic samples were cleaned with alternating acid and base rinses, using 1.5 *N* HCl and 1.0 *N* NaOH, and rinsed with deionized water to remove any adhered organic acids and carbonate in the sample. Eight to twelve milligrams of car-

TABLE 2

Measured Sr isotopic ratios and calculated salinity and delta flow for carbonate samples from sediment cored in Richardson Bay

| Sample | Depth cm | Rb ppm | Sr ppm | 87Sr/86Sr# | Δ87Sr* | Salinity per mil | Delta flow 1000m3/s |
|---|---|---|---|---|---|---|---|
| **Gravity Core** | | | | | | | |
| RBGC-3 | 30 | 0.36 | 1634 | 0.709165 (2) ± 5 | -3.3 | 22.10 ± 2.5 | 1.71 ± 0.79 |
| RBGC-4 | 40 | 0.47 | 1389 | 0.709198 (2) ± 9 | -0.7 | 31.14 ± 5.0 | 0.27 ± 0.27 |
| RGGC-5 | 50 | 0.48 | 1676 | 0.709168 (2) ± 8 | -3.7 | 21.15 ± 2.3 | 2.02 ± 0.81 |
| RBGC-7 | 70 | 0.13 | 1827 | 0.709203 (2) ± 12 | 0.5 | 38.40 ± 7.7 | 0.04 ± 0.04 |
| RBGC-9 | 90 | 0.34 | 1395 | 0.709193 (2) ± 14 | -0.5 | 32.15 ± 5.4 | 0.22 ± 0.22 |
| RBGC-10 | 100 | 0.14 | 1594 | 0.709213 (2) ± 5 | 0.8 | 40.77 ± 8.8 | 0.02 ± 0.02 |
| RBGC-12 | 120 | 0.06 | 1533 | 0.709201 (2) ± 5 | -0.4 | 32.69 ± 5.6 | 0.19 ± 0.19 |
| RBGC-13 | 130 | 0.21 | 1878 | 0.709169 (2) ± 5 | -2.9 | 23.13 ± 2.7 | 1.42 ± 0.76 |
| RBGC-14 | 140 | 0.40 | 2088 | 0.709197 (2) ± 5 | -0.1 | 34.39 ± 6.2 | 0.13 ± 0.13 |
| RBGC-15 | 150 | 0.45 | 1901 | 0.709167 (2) ± 20 | -3.1 | 22.60 ± 2.6 | 1.56 ± 0.78 |
| RBGC-16 | 160 | 0.77 | 1527 | 0.709182 (1) ± 10 | -1.6 | 27.28 ± 3.8 | 0.62 ± 0.52 |
| RBGC-17 | 170 | 0.30 | 2099 | 0.709183 (2) ± 5 | -1.5 | 27.66 ± 3.9 | 0.58 ± 0.49 |
| RBGC-18 | 180 | 0.82 | 1529 | 0.709158 (2) ± 7 | -4.0 | 20.49 ± 2.1 | 2.26 ± 0.81 |
| RBGC-19 | 185 | 0.65 | 2087 | 0.709143 (2) ± 5 | -5.5 | 17.74 ± 1.6 | 3.46 ± 0.80 |
| RBGC-20 | 195 | 0.33 | 1915 | 0.709174 (2) ± 9 | -2.4 | 24.57 ± 3.1 | 1.07 ± 0.69 |
| **Long Core** | | | | | | | |
| RB-2.1A | 417 | 0.35 | 1620 | 0.709187 (2) ± 7 | -1.1 | 29.3 ± 4.4 | 0.41 ± 0.38 |
| RB-2.2A | 526 | 0.54 | 1535 | 0.709181 (2) ± 5 | -1.7 | 26.9 ± 3.7 | 0.67 ± 0.54 |
| RB-2.3A | 608 | - | - | 0.709163 (1) ± 10 | -3.5 | 21.6 ± 2.4 | 1.87 ± 0.80 |
| RB-2.4A | 666 | 0.22 | 1465 | 0.709157 (2) ± 14 | -4.1 | 20.3 ± 2.1 | 2.34 ± 0.82 |
| RB-2.5A | 724 | 0.41 | 1784 | 0.709179 (2) ± 6 | -1.9 | 26.2 ± 3.5 | 0.78 ± 0.59 |
| RB-2.6A | 849 | - | - | 0.709181 (2) ± 18 | -1.7 | 26.9 ± 3.7 | 0.67 ± 0.54 |
| RB-2.7A | 888 | - | - | 0.709181 (1) ± 10 | -1.7 | 26.9 ± 3.7 | 0.67 ± 0.54 |
| RB-2.10A | 1128 | - | - | 0.709146 (2) ± 7 | -5.2 | 18.2 ± 1.7 | 3.22 ± 0.80 |

# Number of mass spectrometer analysis for each sample is shown in parentheses. * Uncertainty on all $\Delta^{87}Sr$ values is $\pm 1$ based on repeat analyses of standards.

TABLE 3

Measured Sr isotopic ratios and calculated salinity and delta flow for carbonate samples from sediment cored in San Pablo Bay

| Sample | Depth (cm) | 87Sr/86Sr# | Δ87Sr* | Salinity permil | Delta flow 1000m3/s |
|---|---|---|---|---|---|
| **Long Core** | | | | | |
| HF-4cc | 274 | 0.709154 (2) ± 9 | -4.4 | 19.7 ± 2.0 | 1.14 ± 0.22 |
| HF-5-2 | 334 | 0.709176 (2) ± 9 | -2.2 | 25.2 ± 3.3 | 0.59 ± 0.28 |
| HF-6-1B | 380 | 0.709173 (1) ± 9 | -2.5 | 24.3 ± 3.0 | 0.68 ± 0.27 |
| HF-6-1 | 395 | 0.709146 (1) ± 9 | -5.2 | 18.2 ± 1.7 | 1.30 ± 0.20 |
| HF-6-1A | 411 | 0.709138 (1) ± 10 | -6.0 | 17.0 ± 1.5 | 1.46 ± 0.19 |
| HF-6-2 | 426 | 0.709158 (2) ± 8 | -4.0 | 20.5 ± 2.1 | 1.05 ± 0.23 |
| HF-6-2A | 442 | 0.709147 (1) ± 10 | -5.1 | 18.4 ± 1.7 | 1.28 ± 0.21 |
| HF-6-3 | 456 | 0.709137 (2) ± 5 | -6.1 | 16.8 ± 1.4 | 1.48 ± 0.19 |
| HF-6cc | 486 | 0.709161 (1) ± 7 | -3.7 | 21.2 ± 2.3 | 0.98 ± 0.24 |
| HF-7-1 | 517 | 0.709138 (2) ± 5 | -6.0 | 17.0 ± 1.5 | 1.46 ± 0.19 |
| HF-7-1B | 503 | 0.709128 (1) ± 10 | -7.0 | 15.6 ± 1.2 | 1.64 ± 0.17 |
| HF-7-2 | 547 | 0.709133 (2) ± 10 | -6.5 | 16.3 ± 1.3 | 1.55 ± 0.18 |
| HF-7-3 | 578 | 0.709145 (2) ± 5 | -5.3 | 18.1 ± 1.7 | 1.32 ± 0.20 |
| HF-7-3A | 594 | 0.709124 (1) ± 10 | -7.4 | 15.2 ± 1.2 | 1.71 ± 0.17 |
| HF-8-1 | 638 | 0.709139 (2) ± 7 | -5.9 | 17.1 ± 1.5 | 1.44 ± 0.19 |
| HF-8-1B | 625 | 0.709131 (1) ± 10 | -6.7 | 16.0 ± 1.3 | 1.59 ± 0.18 |
| HF-8-3 | 699 | 0.709156 (2) ± 16 | -4.2 | 20.1 ± 2.1 | 1.09 ± 0.22 |
| HF-8cc | 730 | 0.709131 (2) ± 13 | -6.7 | 16.0 ± 1.3 | 1.59 ± 0.18 |
| HF-9-1 | 760 | 0.709141 (2) ± 7 | -5.7 | 17.4 ± 1.5 | 1.40 ± 0.19 |
| HF-9-2 | 790 | 0.709142 (2) ± 12 | -5.6 | 17.6 ± 1.6 | 1.38 ± 0.20 |
| HF-9-3 | 821 | 0.709147 (2) ± 5 | -5.1 | 18.4 ± 1.7 | 1.28 ± 0.21 |
| HF-9cc | 851 | 0.709138 (2) ± 15 | -6.0 | 17.0 ± 1.5 | 1.46 ± 0.19 |
| HF-10-1 | 882 | 0.709142 (2) ± 5 | -5.6 | 17.6 ± 1.6 | 1.38 ± 0.20 |
| HF-10-3 | 942 | 0.709154 (1) ± 10 | -4.4 | 19.7 ± 2.0 | 1.14 ± 0.22 |
| HF-10cc | 973 | 0.709149 (1) ± 7 | -4.9 | 18.7 ± 1.8 | 1.24 ± 0.21 |
| HF-11-1 | 1003 | 0.709145 (2) ± 7 | -5.3 | 18.1 ± 1.7 | 1.32 ± 0.20 |
| HF-11-2 | 1034 | 0.709146 (1) ± 10 | -5.2 | 18.2 ± 1.7 | 1.30 ± 0.20 |
| HF-11-3 | 1064 | 0.709138 (1) ± 10 | -6.0 | 17.0 ± 1.5 | 1.46 ± 0.19 |
| **Gravity Core** | | | | | |
| SPB-3A-2 | 21 | 0.709161 (1) ± 10 | -3.7 | 21.2 ± 2.3 | 0.81 ± 0.19 |
| SPB-3A-3 | 41 | 0.709127 (1) ± 10 | -7.1 | 15.5 ± 1.2 | 1.37 ± 0.14 |
| SPB-3A-6 | 101 | 0.709173 (1) ± 8 | -2.5 | 24.3 ± 3.0 | 0.56 ± 0.22 |
| SPB-3A-7 | 121 | 0.709164 (1) ± 10 | -3.4 | 21.9 ± 2.4 | 0.75 ± 0.20 |
| SPB-3A-8 | 141 | 0.709144 (1) ± 10 | -5.4 | 17.9 ± 1.6 | 1.11 ± 0.16 |
| SPB-3A-9 | 147 | 0.709162 (1) ± 8 | -3.6 | 21.4 ± 2.3 | 0.79 ± 0.20 |
| SPB-3A-10 | 171 | 0.709148 (1) ± 9 | -5.0 | 18.6 ± 1.8 | 1.04 ± 0.17 |
| SPB-3A-11 | 191 | 0.709169 (1) ± 10 | -2.9 | 23.1 ± 2.7 | 0.65 ± 0.21 |

# Number of mass spectrometer analysis for each sample is shown in parentheses. * Uncertainty on all $\Delta^{87}Sr$ values is ±1 based on repeat analyses of standards.

bonate, and 1–4 mg of organic carbon, were graphitized using standard techniques [18], and the $^{14}C/^{12}C$ ratio was measured by accelerator mass spectrometry [19].

For Sr isotopic analyses, mollusk shells (several fragments or whole shells) were cleaned ultrasonically in deionized water, and oven-dried. The whole shells or several shell fragments were powdered, in order to homogenize and average out any seasonal bias that may exist in one small shell fragment. From this powder, a 1–5 mg split was taken and dissolved in weak acetic acid for isotopic analysis. The acetic acid solution was evaporated under a heat lamp and the sample redissolved in 1.5 *N* HCl. One aliquot of the carbonate sample was used to determine Sr and Rb concentrations by isotope dilution using a spike solution of $^{84}Sr$ and $^{85}Rb$. Another aliquot was passed through an ion-exchange column to separate purified Sr for isotopic analysis.

An essential part of this study is the high-precision isotopic ratio measurements of Sr, which are accomplished using a multicollector mass spectrometer with peak switching by magnetic scanning [see 7]. The $\Delta^{87}Sr$ notation is used [20]:

$$\Delta^{87}Sr = \left\{\left(^{87}Sr/^{86}Sr_{sample}\right) - \left(^{87}Sr/^{86}Sr_{standard}\right)\right\} \times 100{,}000$$

The EN-1 seawater standard, prepared by the U.S. Geological Survey, was measured to have an $^{87}Sr/^{86}Sr$ ratio of 0.709198 during part of this study; after adjustments were made to the ion collector system, the mean value decreased to 0.709187. Most samples were measured twice, and the $\Delta^{87}Sr$ values are referenced to the appropriate value of the EN-1 standard. The reproducibility of measurements based on two analyses of the same sample solution is estimated to be $\pm 0.000010$ in the $^{87}Sr/^{86}Sr$ ratio, or $\pm 1$ unit of the $\Delta^{87}Sr$ value, as determined from measurements of standards. The statistically determined uncertainties vary between $\pm 0.5$ and $\pm 1.5$ units of $\Delta^{87}Sr$.

## 6. Results

### *6.1 Radiocarbon ages*

In the cores from San Pablo Bay, which has an abundance of plant remains, seeds and woody material, several radiocarbon ages of organic carbon were the same, within the analytical uncertainty, as those from coexisting carbonate, but others were much higher, by up to several thousand years. Much of the organic carbon was probably transported from the watershed to the bay by way of the Sacramento, San Joaquin, Napa and Petaluma rivers. The organic material from the Richardson Bay gravity core, which is fine grained and amorphous, has consistently older radiocarbon ages than coexisting carbonates; it may be a combination of older detrital organic material of marine origin that is carried through the Golden Gate by tidal currents, and the finer riverine organic fraction. Because the ages of most of the organic carbon samples from both locations are consistently older (by hundreds to thousands of years) than those determined from coexisting carbonate we believe the carbonate ages to be a more accurate representation of the depositional age (Table 1).

Radiocarbon ages must be converted to 'calendar' ages [21–23] due to variations in the carbon cycle and production rate of $^{14}C$ in the atmosphere. However, additional correction is necessary along the west coast of North America and in San Francisco Bay estuary, due to the depletion of $^{14}C$ in Pacific Ocean coastal water. The radiocarbon age of Pacific Ocean coastal water is affected by the mixing of surface water with intermediate water that has a 'reservoir' $^{14}C$ age of up to 2000 yrs [24]. The old age of the intermediate water carbon is due to its origin in the Atlantic Ocean [25]. Because of exchange between surface and intermediate water, and upwelling off the coast of North America, the seawater end member in San Francisco Bay estuary has a 'reservoir age' of about 625 yrs [26,27]. The $^{14}C$ in river water entering the bay is closer to that of the atmosphere [28]. Radiocarbon measurements of San Francisco Bay dissolved carbon show that the distribution of radiocarbon in the bay as a function of salinity is non-conservative; the intermediate-salinity water is depleted in $^{14}C$ relative to that calculated for simple mixing between the two end members [28]. Using the mixing curve derived by Spiker [28], we estimate that the typical bicarbonate in San Francisco Bay has an average $^{14}C$ reservoir age of 600 yrs for Richardson Bay, and 550 yrs for San Pablo Bay,

using average salinities of 24‰ and 15–20‰ respectively. We have subtracted these reservoir ages from the calendar ages of the carbonates and called them 'corrected ages' (Table 1). For samples containing bomb-produced carbon, an equivalent correction was made by adding 70‰ to the measured $\Delta^{14}C$ value, although this correction is negligible in terms of its effect on the corrected age.

The corrected ages were screened for stratigraphic consistency, and the age–depth data were fit with smooth curves to obtain an age model for the sediments (Fig. 6). Because of the relatively large corrections applied to the data, we do not consider the absolute values of the ages to be more accurate than about $\pm 100$ yrs. Relative ages are somewhat better constrained.

### 6.2 *Strontium isotopic data*

Strontium isotopic compositions and depth in core for Richardson Bay and San Pablo Bay samples are listed in Tables 2 and 3 and summarized in Fig. 5. For Richardson Bay, the $\Delta^{87}Sr$ values fall between 0 and about $-5$. In the shallow core there is a discernable trend, with higher values in the 70–120 cm depth range than in the 150–200 cm depth range. In the deeper core five of the analyses yield $\Delta^{87}Sr$ values similar to those expected for growth in the modern environment ($-2$ to $-3$), whereas two analyses at the 600–670 cm depth and one from the 1120 cm depth give lower $\Delta^{87}Sr$ values. For San Pablo Bay, the $\Delta^{87}Sr$ values are between $-2$ and $-7.5$ (modern $\Delta^{87}Sr$ values are $-4$ to $-6$). The values from the shallow San Pablo Bay core are generally equal to or lower than the modern value; the deeper core has relatively high values in the upper part, and almost uniformly low values in the remainder of the core. The $\Delta^{87}Sr$ values are lowest in the depth interval 500–620 cm.

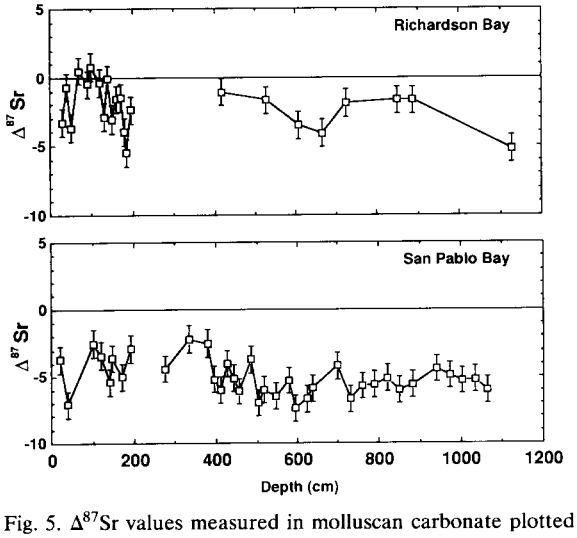


Fig. 5. $\Delta^{87}Sr$ values measured in molluscan carbonate plotted against depth in core (cm) for (top) Richardson Bay gravity core and long core and (bottom) San Pablo Bay gravity core and long core.

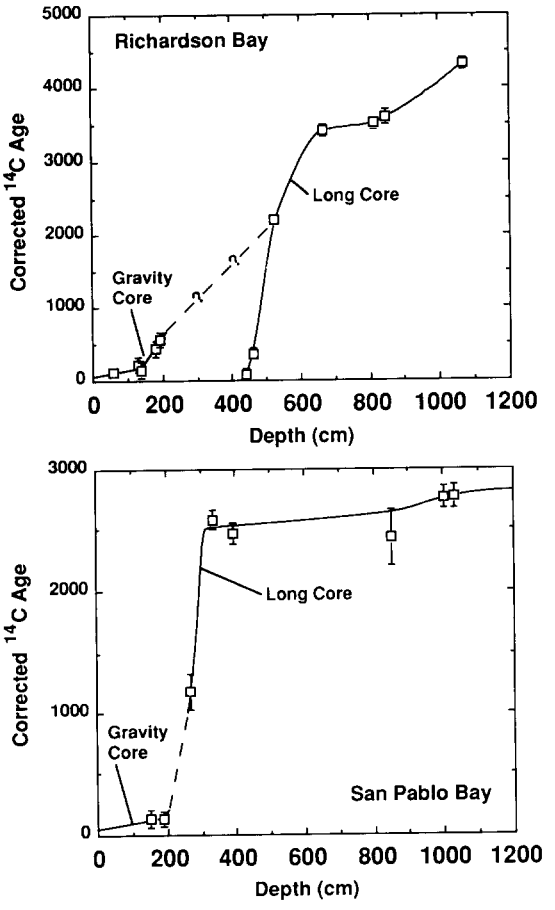


Fig. 6. (top) Sediment thickness (cm) versus corrected radiocarbon age (yrs B.P.) for Richardson Bay gravity and long core. (bottom) Sediment thickness versus corrected radiocarbon age for San Pablo Bay core (Hamilton Field).

## 7. Discussion

### 7.1 Sedimentation rates

Radiocarbon dates from both the deep cores and the gravity cores from Richardson and San Pablo bays indicate that sedimentation rates varied substantially over the past 4300 yrs (Fig. 6). In Richardson Bay, sedimentation rates were highest in the long core between 680 and 1070 cm, 3400–4300 yrs ago ($4.4 \pm 0.4$ mm/yr), and between 0 and 120 cm in the gravity core, 0–200 yrs ago ($6 \pm 3$ mm/yr). The average sedimentation rate is $2.5 \pm 0.1$ mm/yr for the long core and $3.4 \pm 0.6$ mm/yr for the gravity core. In the San Pablo Bay cores the sedimentation rates were much higher, presumably because San Pablo Bay is closer to the mouth of the Sacramento–San Joaquin rivers (Fig. 1). The highest sedimentation rates are indicated by the oldest section of the core, between 334 and 1034 cm ($25 \pm 5$ mm/yr). The average sedimentation rate in the gravity core is $14 \pm 7$ mm/yr. A similar pattern is observed in the Richardson Bay long core, but there is a possibility that the 'young' age of the core material near the top of the cored interval is a consequence of caving of near-surface sediment into the hole [16].

### 7.2 Paleosalinity and paleodischarge

For both salinity and delta flow, the data are compared to hypothetical modern 'normal' values. The actual modern average delta flow is roughly 600 $m^3/s$, which is estimated to be 50–60% of what it would be if there were no water diverted for agricultural and other uses [29]. We have therefore chosen the value of 1100 $m^3/s$ as the 'modern diversion-corrected normal' value for use in discussion of paleoclimate.

Paleosalinities, calculated from $\Delta^{87}Sr$ using the relationship shown in Fig. 4, are shown as a function of time in Fig. 8–10. For all calculations we assume a constant salinity–Sr isotopic relationship. For the Richardson Bay record (Figs. 8 and 10), the data indicate relatively high salinity at about 40, 140–210, 270, 2100 and 3450–3700 yrs B.P., and relatively low salinity at about 80, 220, 310, 440–500, 3100–3400 and 4300 yrs B.P.

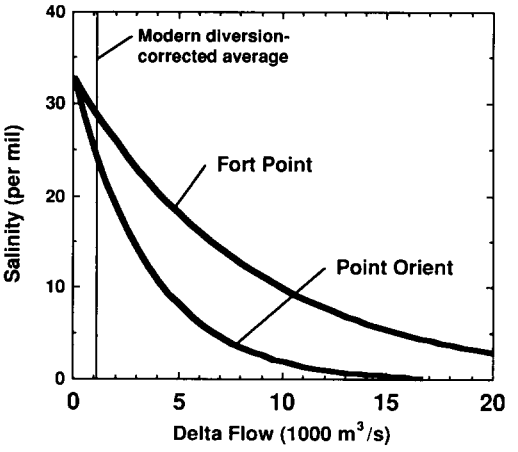


Fig. 7. Salinity versus delta flow for salinity monitoring stations at Point Orient, located in west San Pablo Bay, and Fort Point, located near the Golden Gate [from 10]. Localities of salinity monitoring stations are shown in Fig. 1.

In the San Pablo Bay record (Fig. 9), salinity was higher than modern from 90–110, 155 and 2510–2530 yrs B.P.; low salinity is indicated for ca. 50 and 2550–2650 yrs B.P.

There may be a slight seasonal bias in the way the $\Delta^{87}Sr$, and therefore paleosalinity, is recorded in the mollusk shells, as a result of seasonal variations in the calcification rates during shell formation. Field studies of growth rates of *Macoma balthica* in San Francisco Bay show that the rate of increase in shell length is depends mainly on food supply (planktic and benthic microalgae) [30]. In the north bay (between the Golden Gate and the delta, Fig. 1), growth of *M. balthica* occurs during every month of the year except January, and peaks in early summer and fall (during both high and low flow regimes). Growth of the clam is unrelated to salinity [30]. Hence, we assume that the fossil shell samples used in this study (which were mostly *Macoma* species) are representive of annual average salinity, with no bias toward higher or lower salinity seasons. Work in progress, with isotopic measurements of the growth layers across a single shell, will more directly address this issue.

The conversion of the salinity data to paleodischarge (or 'delta flow') of the Sacramento–San Joaquin river system requires knowledge of the relationship between salinity and delta flow, which

is a function of position within the estuary and of the paleobathymetry of the bay. In general, for a given water depth the salinity in the bay is primarily a function of the distance upstream from the mouth of the bay, and except at very high flows is much less strongly dependent on depth in the water column at each point [10]. The best-fit relationships between surface-water salinity and delta flow over a 40 yr period [10] are shown (Fig. 7) for two sites close to our core locations: Fort Point is near Richardson Bay, and Point Orient is near western San Pablo Bay. In general, sites close to the Golden Gate, such as Fort Point, show relatively small changes in $\Delta^{87}Sr$ (2 units) for typical delta flows between 500 and 2500 $m^3/s$. Better salinity resolution is possible using the San Pablo Bay sites, which have somewhat more sensitivity than shown by the curve for Poiknt Orient, some 12 units of $\Delta^{87}Sr$ variation for the same range of delta flow values.

We used two slightly different approaches to convert salinity data to delta flow. For the San Pablo Bay sites, the exponential relationships between salinity and delta flow proposed by Peterson [10] were used, with the exponential coefficient adjusted so that the salinity at the long core site would be 20‰, and the salinity at the gravity core site 18‰ for a 'normal' delta flow of 1100 $m^3/s$. The 'normal' salinity values associated with 1100 $m^3/s$ delta flow are approximate, and in-

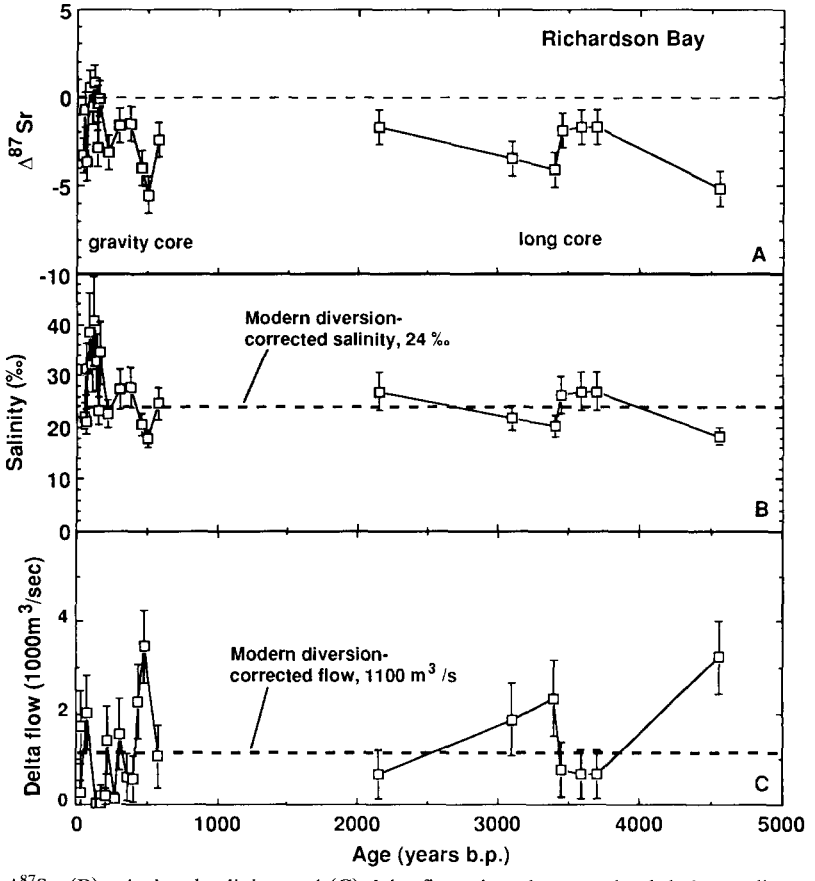


Fig. 8. (A) Measured $\Delta^{87}Sr$, (B) calculated salinity, and (C) delta flow plotted versus depth below sediment–water interface for Richardson Bay gravity core and long core. The modern diversion-corrected salinity, $\Delta^{87}Sr$, and delta flow in Richardson Bay are shown for comparison. The 'average' salinity in Richardson Bay, based on measurements over the past 30 yrs, is approximately 24‰ (plotted with dashed line in (B) for comparison), with a corresponding $\Delta^{87}Sr$ of −2 (plotted with dashed line in (A)). The estimated pre-diversion delta flow is 1100 $m^3/c$, also plotted with a dashed line, in (C)).

ferred from the values observed at nearby USGS monitoring sites [31,32]. For the Richardson Bay sites, we used a polynomial fit to the published data for the Alameda monitoring station, which shows a salinity–delta flow relationship similar to the Richardson Bay area [31,32]. The polynomial fit was used in preference to the exponential fit to obtain a more realistic relationship for high salinity values; at salinities below 30‰ the same results are obtained from the exponential fit.

A detailed analysis of the effect of changing water depth of San Francisco Bay on the salinity–delta flow relationship is not possible at the moment, but will be pursued as part of continuing studies. We can place limits on the effects of changing estuarine paleobathymetry by relating the salinity–flow function to the volume of the bay between the sampling site and the delta. As shown in Fig. 2, sea level may have risen by 5–10 m over the past 5000 yrs. Using an average sedimentation rate of 1–2mm/yr in the bay, over the same time period, about 5–10 m of sediment would have accumulated. The volume of the bay may therefore not have changed much as a result of sedimentation over this time period. However, because the delta progrades (indicated by high-resolution seismic reflection profiles from the east side of San Pablo Bay [P. Williams, pers. commun.]) the volume of the bay upstream of any sampling point decreases with time. Consequently, in the past, the volume of the bay upstream of our sample localities was larger. Using the modern salinity versus flow relationships therefore probably causes us to underestimate paleodelta flow.

The calculated delta flow values are shown in Figs. 8, 9 and 10. The uncertainty in calculated delta flow shown in the figures is only that associated with the $\pm 1$ unit uncertainty in the measurement of $\Delta^{87}Sr$. The other uncertainities are not included, to preserve clarity. The absolute values of the flows will be subject to some revision, but the relative highs and lows will not change. According to our models, the periods of low salinity correspond to average annual delta flow values of about 1500 $m^3/s$ in San Pablo Bay and 1500–3000 $m^3/s$ in Richardson Bay; these numbers are 2–5 $\times$ times the present value of about 600$m^3/s$. The delta flows corresponding to the periods of high salinity in Richardson Bay are

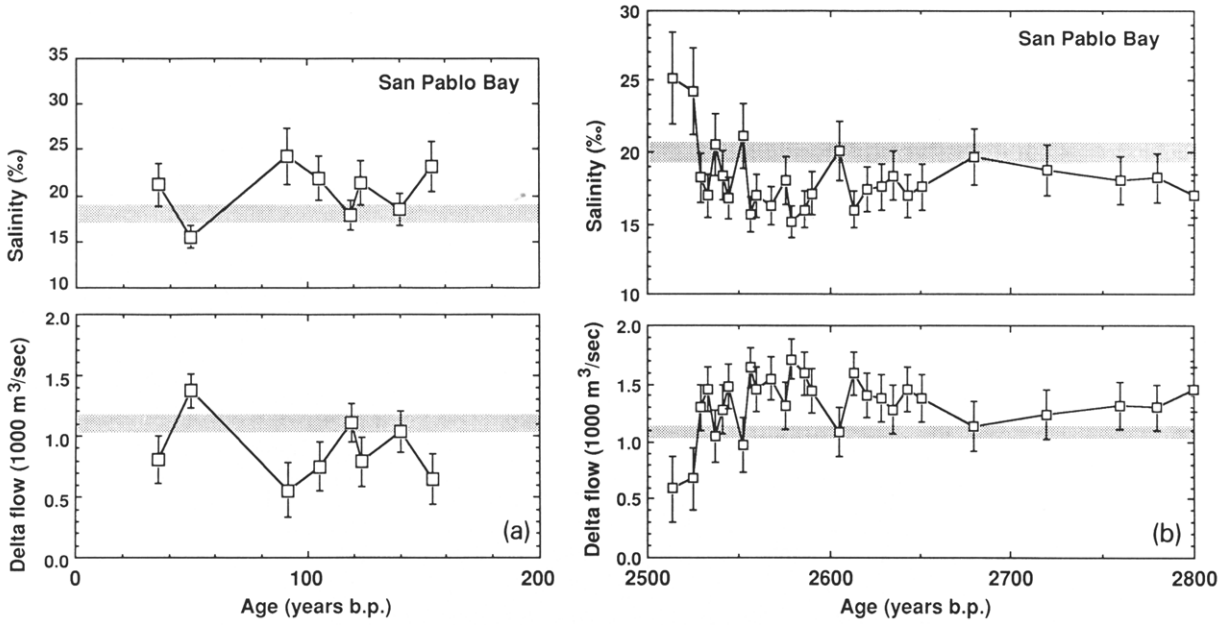


Fig. 9. (a) Salinity and delta flow plotted against corrected radiocarbon age for San Pablo Bay gravity core. (b) Salinity and delta flow plotted against corrected radiocarbon age for San Pablo Bay long core. Modern diversion-corrected salinity and delta flow are shown for comparison.

poorly constrained, but appear to be less than 500 $m^3/s$. In San Pablo Bay, where salinity and delta flow are better constrained, the lower salinity values convert to delta flows between 550 and 800$m^3/s$.

With the exception of the data from Richardson Bay for the 40, 140–210 and 270 yr B.P. intervals, most of the data suggest that the natural salinity was lower, indicating that the natural river discharge into the bay was higher (in comparison to the estimated diversion-corrected 'normal' values) over much of the past 4300 yrs. Furthermore, our methods of estimating both paleosalinity and paleodischarge should be biased toward underestimating the paleodischarge. Consequently, the 4300 yr average river discharge into the bay could be substantially higher than the estimated modern diversion-corrected value, and the 4300 yr average salinity in the bay would be correspondingly lower. More extensive data and more detailed modelling will be necessary to refine these inferences.

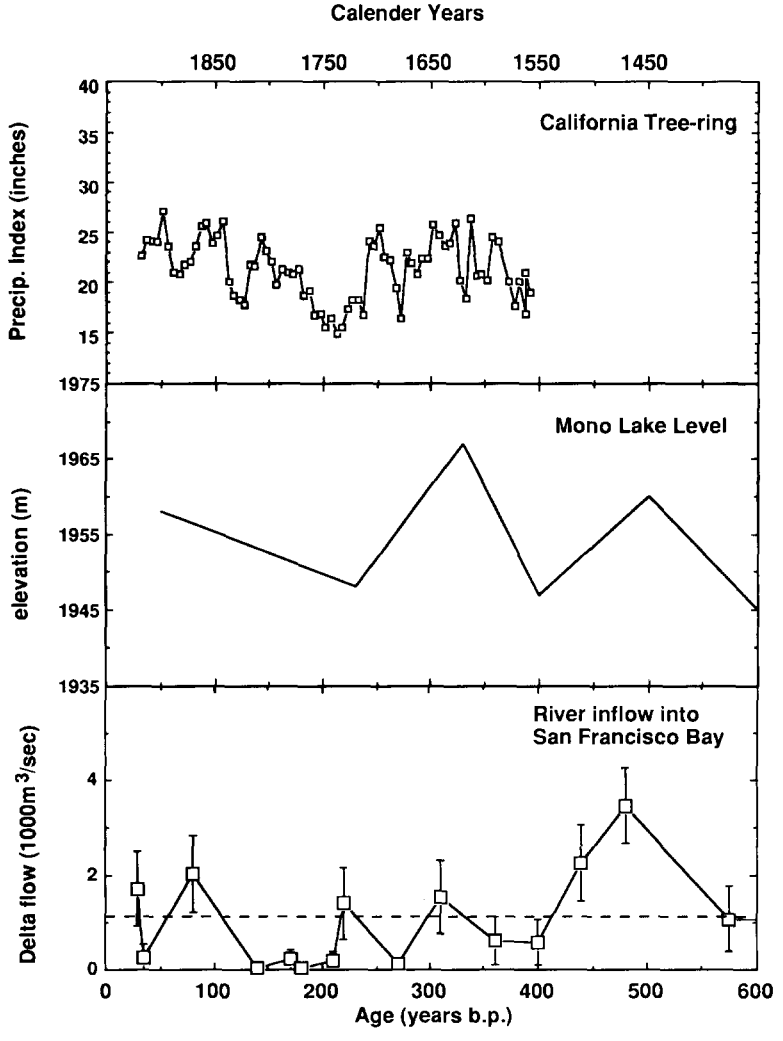


Fig. 10. Inferred delta flow into San Francisco Bay over the past 600 yrs (calculated from $\Delta^{87}Sr$ paleosalinity in this study), plotted against corrected radiocarbon age for Richardson Bay gravity core (bottom) compared with the precipitation index from treering width data from northern California [1], and freshwater inflow record from paleo-lake level data from Mono Lake [6]. Correlation between the three records is imprecise due to the large age correction needed for San Francisco Bay carbonate samples (see text).

The data are insufficient for establishing the frequency and amplitude of cyclicity in the salinity–discharge record. However, the data from the shallow Richardson Bay core indicate that major salinity changes can occur on timescales shorter than 100 yrs. The period from 150 to 500 yrs B.P. exhibits the total range in $\Delta^{87}Sr$ seen in the record back to 4300 yrs B.P.

### *7.3 Comparison with other paleoclimate records*

Our inferred delta flow values for the past 600 yrs (Richardson Bay data) are compared with other paleoclimatic records (Fig. 10). This comparison is limited by the large uncertainty in correcting the radiocarbon ages of the carbonate shells. Reasonably good correspondence is apparent, however, and all three records have some evidence for quasi-cyclical variations of about 200 yrs in period. Climatic variations with 88 and 200 yr periodicity, measured using cosmogenic $^{10}Be$ in ice cores [33] and varved lake sediments [34,35], have been attributed to fluctuations in solar activity as recorded in the production rate of $^{14}C$ [36]. The period of extremely low delta flow between 210 and 140 ys B.P. (1740–1810 B.C.) in San Francisco Bay (Fig. 10) corresponds to a period of extended drought recorded in treerings from the western United States [1,2]. Treeline variations in the White Mountains of eastern California indicate cooler and wetter conditions than modern between 4200 yrs and 2000 yrs B.P., becoming cooler and drier between 2000 yrs B.P. and the present [5]. Our paleosalinity data also suggest that average river inflow was higher than modern (pre-diversion) prior to 2000 yrs ago, and therefore can be considered to be in agreement with the treeline data. Mono Lake was also significantly larger at ca. 3800 yrs B.P. [6], indicating higher precipitation. Our data indicate a peak wet period at about 3400 and 4300 yrs B.P., but this difference in age could be due to inherent uncertainties in the dating method rather than to a real difference.

## 8. Summary

$^{87}Sr/^{86}Sr$ measurements of fossil carbonate shells separated from cores from San Francisco Bay show that the salinity (and inferred freshwater inflow) has fluctuated substantially in the past. Over the past 600 yrs and at ca. 2600 and 3400 yrs B.P. a cycle time of about 200 yrs may be present, but this requires further investigation. There appears to be a longer term trend toward higher salinity (lower freshwater input) from 2500–4300 yrs ago to the present, even allowing for the effects of diversion. Comparison of these results to those of other terrestrial paleoclimate records (treering widths, treeline elevation and lake levels) is hampered by uncertainties in age determinations, but there is reasonable agreement nevertheless.

The use of strontium isotopic measurements in estuarine sediments for paleoclimatic and water resource assessment should be applicable in other estuarine and deltaic settings worldwide, both modern and ancient. This type of data could contribute substantially to the understanding of the natural temporal variability in the amount of precipitation and streamflow along continental margins, allowing a greater understanding of variations in the hydrologic cycle, both spatially and temporally. Other types of climatic events that might be recorded by strontium isotopic measurements in the sedimentary record include monsoons, meltwater events, drought and floods, and El Niños.

## Acknowledgements

This work was started as B.L. Ingram's Ph.D thesis at Stanford University. We thank J.C. Ingle, D. Sloan, D. Peterson, Y. Kolodny, S.C. Brassell, J. Stebbins and M. McWilliams for advice regarding the research, and S.M. Savin and an anonymous reviewer for providing insightful reviews of the manuscript. We also thank H.E. Clifton, R. Anima and A. van Geen of the U.S. Geological Survey for providing some of the core material used in this study. Ray Solbau of the Lawrence Berkeley Laboratory, John Christensen and John Lassiter helped drill cores at Hamilton Field. We thank J.R. Southon, S. Trumbore and M. Kashgarian of the Lawrence Livermore National Laboratory for their assistance with the AMS radiocarbon dating and data reduction. This work was supported by the Director, Office of Energy Research, Office of Basic Energy Sciences, Engineering and Geosciences Division of

the U.S. Department of Energy under contract DE-AC03-76SF00098.

## References


1 H.C. Fritts, Tree-ring evidence for climatic changes in western North America, Mon. Weath. Rev. 93, 421–443, 1965.

2 H.C. Fritts, G.R. Lofgren and G.A. Gordon, Variations in climate since 1602 as reconstructed from tree rings, Quat. Res. 12, 18–46, 1979.

3 L.J. Graumlich, Precipitation variation in the Pacific Northwest (1675–1975) as reconstructed from tree rings, Ann. Assoc. Am. Geogr. 77, 19–29, 1987.

4 V.C. Lamarche, Chronologies from temperature-sensitive bristlecone pines at upper treeline in western United States, Tree-Ring Bull. 34, 21–45, 1974.

5 V.C. Lamarche, Holocene climatic variations inferred from treeline fluctuations in the White Mountains, California, Quat. Res. 3, 632–660, 1973.

6 S. Stine, Late Holocene fluctuations of Mono Lake, eastern California, Palaeogeogr., Palaeoclimatol., Palaeoecol. 78, 333–381, 1990.

7 B.L. Ingram, Paleoclimatic and paleoceanographic studies of estuarine and marine sediments using strontium isotopes, Ph.D Dissert., Stanford Univ., 1992.

8 B.L. Ingram and D. Sloan, Strontium isotopic composition in estuarine sediments as paleosalinity and paleoclimate indicator, Science 255, 68–72, 1992.

9 D.R. Cayan and D.H. Peterson, The influence of north Pacific atmospheric circulation on streamflow in the west, in: Aspects of Climate Variability in the Pacific and the Western Americas, D.H. Peterson, ed., AGU Geophys. Monogr. 55, 375–398, 1989.

10 D.H. Peterson, R.C. Cayan, J.F. Festa, F.H. Nichols, R.A. Walters, J.V. Slack, S.E. Hager and L.E. Schemel, Climate variability in an estuary: effects of riverflow on San Francisco Bay, in:. Aspects of Climate Variability in the Pacific and the Western Americas, D.H. Peterson, ed., AGU Geophys. Monogr. 55, 419–442, 1989.

11 B.F. Atwater, C.W. Hedel and E.J. Helley, Late Quaternary depositional history, Holocene sea-level changesand vertical crustal movement, southern San Francisco Bay, California, U.S. Geol. Surv. Prof. Pap. 1014, 15 pp., 1977.

12 B.F. Atwater, S.G. Conard, J.N. Dowden, C.W. Hedel, R.L. MacDonald and W. Savage, History, landforms and vegetation of the estuary's tidal marshes, in: San Francisco Bay: the Urbanized Estuary, T.J. Conomos, ed., pp. 347–385, Am. Assoc. Adv. Sci., Pac. Div., San Francisco, 1979.

13 B.F. Atwater, B.E. Ross and J.F. Wehmiller, Stratigraphy of late Quaternary estuarine deposits and amino acid stereochemistry of oyster shells beneath San Francisco Bay, California, Quat. Res. 16, 181–200, 1981.

14 R.G. Fairbanks, A 17,000-year glacio-eustatic sea level record: influence of glacial melting rates on the Younger Dryas event and deep-ocean circulation, Nature 342, 637–642, 1989.

15 R.B. Krone, Sedimentation in the San Francisco Bay system, in: San Francisco Bay: the Urbanized Estuary, T.J. Conomos, ed., pp. 85–96, Am. Assoc. Adv. Sci., Pac. Div., San Francisco, 1979.

16 A. Van Geen, S.N. Luoma, C.C. Fuller, R. Amina, H.E. Clifton and S. Trumbore, Evidence from Cd/Ca ratios in foraminifera for greater upwelling off California 4,000 years ago, Nature 358, 54–56, 1992.

17 M.R. Palmer and J.M. Edmond, The strontium isotope budget of the modern ocean, Earth Planet. Sci. Lett. 92, 11–26, 1989.

18 J.S. Vogel, D.E. Nelson and J.R. Southon, $^{14}C$ background levels in an accelerator mass spectrometry system, Radiocarbon 29 (3), 323–333, 1987.

19 J.C. Davis et al., LLNL/UC AMS facility and research program, in: Proc. 5th Int. Conf. Accelerator Mass Spectrometry, Nucl. Instrum. Meth. B52 (3,4), 269–272, 1990.

20 D.J. DePaolo and B.L. Ingram, High-resolution stratgraphy with strontium isotopes, Science 227, 938–941, 1985.

21 M. Stuiver and G.W. Pearson, Calibration of the radiocarbon time scale, 2500–5000 BC, in: Radiocarbon After Four Decades, R.E. Taylor, A. Long and R.S. Kra, eds., pp. 19–33, Springer, 1992.

22 M. Stuiver and G.W. Pearson, High-precision calibration of the radiocarbon time scale, AD 1950–500 BC, in: Proc. 12th Int. $^{14}C$ Conf., Radiocarbon 28 (2B), 805–838, 1986.

23 G.W. Pearson and M. Stuiver, High-precision calibration of the radiocarbon time scale, 500–2500 BC, in: Proc. 12th Int. $^{14}C$ Conf., Radiocarbon 28 (2B), 839–862, 1986.

24 M. Andree, J. Beer, H. Oeschger, A. Mix, W. Broecker, N. Ragano, P. O'Hara, G. Bonani, H.J. Hofmann, E. Morenzoni, M. Nessi, X. Suter and W. Wolfli, Accelerator radiocarbon ages on foraminifera separated from deep-sea sediments, in: The Carbon Cycle, E.T. Sundquist and W.S. Broecker, eds., AGU Geophys. Monogr. 32, 143–153, 1985.

25 W.S. Broecker and T.H. Peng, Tracers in the Sea, Eldigo, Palisades, N.Y., 1977.

26 J.R. Southon, D.E. Nelson and J.S. Vogel, A record of past ocean–atmosphere radiocarbon differences from the northeast Pacific, Paleoceanography 5, 197–206, 1990.

27 M. Stuiver, G.W. Pearsonand T. Braziunas, Radiocarbon age calibration of marine samples back to 9000 cal yr BP, Radiocarbon, 28 (2B), 980–1021, 1986.

28 E.C. Spiker, The behavior of $^{14}C$ and $^{13}C$ in estuarine water: effects of in situ $CO_2$ production and atmospheric exchange, Radiocarbon 22 (3), 647–654, 1980.

29 F.H. Nichols, J.E. Cloern, S.N. Luomaand D.H. Peterson, The modification of an estuary. Science 231, 567–573, 1986.

30 J.K. Thompson and F.H. Nichols, Food availability controls seasonal cycle of growth in *Macoma balthica* (L.) in San Francisco Bay, California, J. Exp. Biol. Ecol. 116, 43–61, 1988.

31 T.J. Conomos, R.E. Smith, D.H. Peterson, S.W. Hager and L.E. Schemel, Processes affecting seasonal distributions of water processes in the San Francisco Bay estuarine system, in: San Francisco Bay: the Urbanized Estuary, T.J. Conomos, ed., pp. 115–142, Am. Assoc. Adv. Sci., Pac. Div., San Francisco, 1979.

32 T.J. Conomos, Properties and circulation of San Francisco Bay waters, in: San Francisco Bay: the Urbanized Estuary, T.J. Conomos, ed., pp. 47–84, Am. Assoc. Adv. Sci., Pac. Div., San Francisco, 1979.

33 J. Beer, U. Siegenthaler, G. Bonani, R.C. Finkel, H. Oesheger, M. Suter and W. Wolfli, Information on past solar activity and geomagnetism from $^{10}$Be in the Camp Century ice core, Nature 331, 675–679, 1988.

34 J.D. Halfman and T.C. Johnson, High-resolution record of cyclic climatic change during the past 4 ka from Lake Turkana, Kenya, Geology 16, 496–500, 1988.

35 R.Y. Anderson, A solar/geomagnetic C-14 climate connection: evidence from mid-Holocene varves in a Minnesota lake, in: 8th PACLIM Workshop, Tech. Rep. 26, Interagency Ecol. Stud. Program, Sacramento–San Joaquin Estuary, 1991.

36 M. Stuiver and P.D. Quay, Changes in atmospheric carbon-14 attributed to a variable sun, Science 207, 11–19, 1980.

37 M. Stuiver and H.A. Polach, Reporting of $^{14}$C data, Radiocarbon 19, 355–363, 1977.